Stanisław Pałubicki Wiesław Czapiewski

The Effect of a Heat Input to the Joint during the Gas Metal Arc Welding of Ferritic-Austenitic Steel 1.4462 on Welding Deformations

Abstract: Welding is a special process, the result of which cannot be fully guaranteed despite the use of all possible and available procedures leading to the correct fabrication of the welded joint. The quality of joints made in the welding process cannot be fully verified during inspection and testing, where any discrepancies may only become apparent during product operation. The tests presented in the article aimed to determine the impact of changes in the value of welding linear energy (heat input) and of correlations between values of process parameters (current, arc voltage and welding rate) on welding deformations of joints made of ferritic-austenitic steel using the GMAW method. The testing methodology, involving the performance of tests based on an experimental scheme, enabled the development of a mathematical model of the test object (MMTO). The analysis of the MMTO revealed its usability in explaining (and forecasting) the mean square deviation of surface flatness (i.e. a parameter used to assess the value of joint flatness deviation) in relation to values of welding process input parameters under specific implementation conditions and assumed significance level $\alpha = 0.05$. The tests revealed the existence of a narrow range of heat input, in relation to which welding deformations were relatively small (as the correlation between welding deformations and the heat input during the welding process was not a monotonic function).

Key words: ferritic-austenitic steel, heat input, linear energy, welding deformations, welded joint macrostructure

DOI: 10.32730/mswt.2024.68.1.4

1. Introduction

The primary purpose of the welding process is the obtainment of permanent welded joints meeting related technical requirements. The material subjected to welding (base material) and the filler metal are brought to the liquid state by means of heat (e.g. welding arc) and, afterwards, undergo solidification (crystallisation) to form the weld [1–3].

In many sectors of the economy (civil engineering, power sector, transport, industrial fittings and medicine), corrosion-resistant steels are used to reduce the rate of the corrosive wear of structural elements and, consequently, to optimise operating costs of structures exposed to aggressive environments. The most commonly used steels are those characterised by the austenitic structure [4–7]. The turn of the 1970s and 1980s saw the growing popularity of ferritic-austenitic (the so-called duplex) steels, characterised by the dual-phase structure (hence the name). In the state of structural equilibrium, obtained as a result of appropriate chemical composition and manufacturing process, the steels are characterised by the fine-grained structure containing approximately 50 % ferrite (α) with the balance being austenite (γ). Ferrite provides the steel with the required resistance to stress corrosion, whereas austenite provides appropriate plastic properties [8–10].

Ferritic-austenitic steels are used in numerous industrial sectors such as [8, 11–14]:

- **oil and gas extraction industry** – used because of their corrosion resistance when exposed to various substances such as CO_2, H_2S, chlorides as well as low-pH compounds and due to high strength; they are used for both coastal and seabed pipelines;
- **chemical industry** – used under corrosion conditions, usually in processes taking place at elevated temperature, in a chloride environment as a substitute for austenitic steel; they are used to make stripping columns, heat exchangers used in the production of high-molecular plastics, pressure vessels for organic compounds as well as tanks and devices for the production of alcohol, sulphuric acid and phosphoric acid;
- **papermaking industry** – used for economic reasons (the use of duplex steel made it possible to reduce the thickness of elements by 35 % in comparison with elements clad with stainless steel, and by 50 % if compared to elements made of non-alloy steels); they are used to make devices for preparing chips and in the chemical pulping of wood and bleaching, thermomechanical processing of pulp and various types of tanks as well as pulp digesters and delignification devices;
- **shipbuilding industry** – because of more favourable mechanical properties if compared to austenitic steels, it is possible to reduce the total weight by approximately 10 % and obtain better resistance to pitting corrosion and crevice corrosion; used in the manufacturing of cargo tanks of chemical tankers intended for the transport of various types of aggressive chemicals;
- **civil engineering** – because of their higher strength, they replace structural steels, thus allowing for the significant

dr inż. Stanisław Pałubicki – Koszalin University of Technology, Faculty of Mechanical Engineering and Power Engineering, Department of Production Engineering; mgr inż. Wiesław Czapiewski – Koszalin University of Technology, Doctoral School

Corresponding author: stanislaw.palubicki@tu.koszalin.pl

reduction of structure weight and the longer service life of elements made of them;
- **seawater desalination plants and flue gas desulphurisation plants**.

Normalised corrosion-resistant steels, including ferritic-austenitic steels, are contained in the PN-EN 10088-1 standard, whereas related technical delivery conditions are specified in the w PN-EN 10088-2 standard.

The notion of welding strains (deformations/distortions) refers to changes in the dimensions and the shape of elements taking place as a result of the welding thermal cycle. The welding process requires a significant heat input, which locally heats elements and melts their edges within a narrow space. An increase in the temperature of elements increases their dimensions, yet the distribution of temperature in elements subjected to joining is not uniform. The base material surrounding the welded joint is heated only to a small extent, which limits the freedom of dimensional changes in the heated zone. The condition triggering the formation of permanent distortions is an increase in temperature sufficiently high so that corresponding thermal strains exceed deformations corresponding to the yield point. Cooling induces the volumetric contraction of metals. Welding shrinkage is significantly greater than the expansion of the material of elements subjected to joining; dimensions of the welded joint decrease, welded elements become shortened and both the longitudinal section and the cross-section of the weld decrease as well. Shrinkage in the direction of weld thickness is uninterrupted, i.e. the weld shrinks freely in this direction and does not trigger internal stresses. Longitudinal shrinkage in the direction of length and transverse shrinkage in the direction of the width of the weld trigger deformations of elements subjected to welding. In butt welded joints of thin elements characterised by low stiffness (e.g. two sheets), transverse shrinkage triggers the loss of flatness, i.e. the formation of distortions, corrugations, warping or the buckling of the plane of joined elements as well as angular deformations (sagging/deflection of elements) [15, 16].

Depending on conditions and production volume, the welding of duplex steels is possible using most welding methods. In industrial practice, due to the automated feeding of the weld metal, the gas-based shielding of the welding area, high efficiency and versatility, the dominant welding method is that involving the use of the arc, consumable electrodes and shielding also known as gas metal arc welding (GMAW). The method is characterised by strong correlations between the thermal field, changes in mechanical properties and the structure of welded joints as well as by the formation of welding stresses and strains [17, 18].

The welding thermal cycle has a significant effect on the structure, phase composition, phase morphology and mechanical properties of welded joints. The parameter enabling the control of the process is linear welding energy, dependent on welding current, arc voltage, welding rate and the thermal efficiency of the process. The issue concerning the determination of heat input (linear welding energy) has been discussed in numerous publications [8, 19–23].

Linear welding energy is a measure expressing the amount of heat per the length unit of the weld [24]. The parameter cannot be measured directly; it is calculated based on measured values of arc voltage, welding current and welding rate using the following dependence (1):

$$Q = k\,\frac{UI}{v} \cdot 10^{-3}, \qquad (1)$$

where Q – linear welding energy [kJ/mm]
k – coefficient of welding process thermal efficiency
U – arc voltage [V]
I – welding current
A and v – welding rate [mm/s]

Values of heat transfer efficiency coefficient k in relation to various welding methods are contained in publication [25].

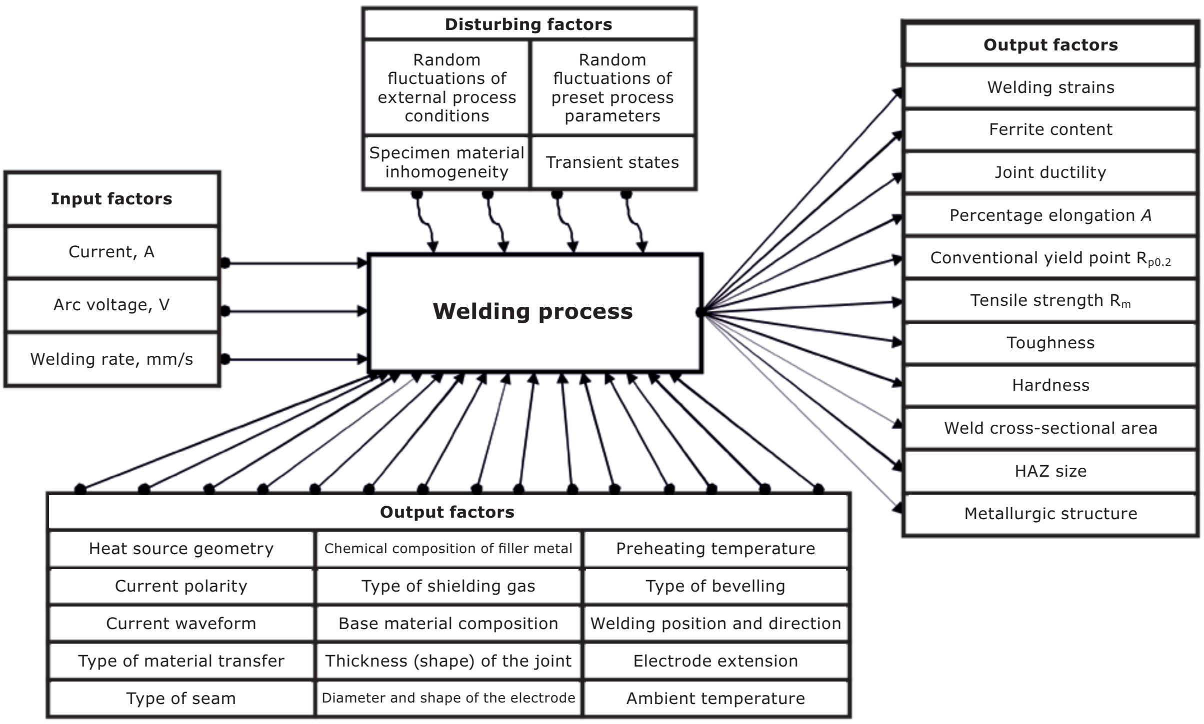

Fig. 1. Schematic diagram of the object of tests

There are only a few research publications containing results and describing the correlation between the structure of joints and their properties and the input parameters of the welding process (current, arc voltage, welding rate, i.e. linear energy) [31]; there is no systemic approach enabling the determination of dependences describing the effect of the above-named input parameters on the obtainability (with a certain probability) of joints characterised by previously assumed properties. The possibility of forecasting values of strains generated during the welding process and the minimisation of their effect on dimensions and stability of structures are essential as regards the quality of welded structures. The formation of welding distortions exceeding permissible values necessitates the performance of additional treatment, entailing higher manufacturing costs.

2. Testing methodology

2.1. Test objective

The objective of the experimental tests was the identification of the effect of changes in linear welding energy values (i.e. a generalised preset welding process parameter calculated based on measured values of input parameters including current, arc voltage and welding rate) on deformations of GMAW joints made of ferritic-austenitic steels.

2.2. Test specimens

The results of the analysis of related reference publications and those of preliminary tests enabled the identification of factors concerning the object of tests and the division of the aforesaid factors into four groups (Fig. 1).

The objects of the tests were single butt joints made of ferritic-austenitic steel using the GMAW method and a robotic welding station.

2.3. Scheme of experimental tests

The experimental tests involved the use of a five-level compositional rotational scheme (Table 1). Rotational schemes satisfy the postulate of independence (of the scheme) from the rotation of the coordinate system in the space of input parameters and enable the identification of a model with variances depending only on the distance from the central point of the experiment. The individual factor levels in the scheme were marked as follows [26]:

- +α – maximum upper level,
- +1 – upper level,
- 0 – central (medium) level,
- –1 – lower level,
- –α – minimum lower level.

Within the test scheme, a total of 20 experiments were planned for three input factors (current, arc voltage and welding rate) (8 in the core of the scheme, 6 in star points and 6 in the centre of the scheme).

2.4. Parameters and values of welding parameters

The variability ranges of previously assumed energy parameters of the welding process involving the making of test joints using the MAG method (DC+) within the test scheme (Table 2) were selected taking into account recommendations specified by the manufacturer of the filler metal and available data found in related reference publications.

Table 1. Scheme of experimental tests of test joints obtained using the MAG Standard method (DC+)

	Experiment number	Coded variable		
		Current [A]	Arc voltage [V]	Welding rate [m/min]
Schedule core	1	–1	–1	–1
	2	+1	–1	–1
	3	–1	+1	–1
	4	+1	+1	–1
	5	–1	–1	+1
	6	+1	–1	+1
	7	–1	+1	+1
	8	+1	+1	+1
Star points	9	+α	0	0
	10	–α	0	0
	11	0	+α	0
	12	0	–α	0
	13	0	0	+α
	14	0	0	–α
Schedule centre	15	0	0	0
	15.1	0	0	0
	15.2	0	0	0
	15.3	0	0	0
	15.4	0	0	0
	15.5	0	0	0

Table 2. Input factors and their variability ranges in tests concerning the effect of changes in linear energy values on selected properties of welded joints made of ferritic-austenitic steel using the MAG (DC+) method

Input factors	Input factor parameters
Weld symbol/ welding position	BW (butt welded joint)/ PA (flat position)
Current [A]	90–180
Arc voltage [V]	17–25
Welding rate [m/min]	0.4–0.8
Flow rate of shielding/ backing gas [l/min]	12/6

The input parameters used when making test welded joints using the MAG (DC+) method in accordance with the experiment scheme are presented in Table 3.

2.5. Test materials

The experimental tests involved the use of sheets (3 mm × 1000 mm × 2000 mm) made of duplex steel grade 2205 in

Table 3. Parameters used in the MAG (DC+) welding of test joints in accordance with the schedule of experimental tests

Experiment no.	Input factors		
	Current [A]	Arc voltage [V]	Welding rate [m/min]
1	108	18.6	0.48
2	162	18.6	0.48
3	108	23.4	0.48
4	162	23.4	0.48
5	108	18.6	0.72
6	162	18.6	0.72
7	108	23.4	0.72
8	162	23.4	0.72
9	180	21.0	0.60
10	90	21.0	0.60
11	135	25.0	0.60
12	135	17.0	0.60
13	135	21.0	0.80
14	135	21.0	0.40
15	135	21.0	0.60
15.1	135	21.0	0.60
15.2	135	21.0	0.60
15.3	135	21.0	0.60
15.4	135	21.0	0.60
15.5	135	21.0	0.60

accordance with AISI, X2CrNiMoN22-5-3, 1.4462 in accordance with PN-EN 10088-2. The producer of the steel sheets was Outokumpu Stainless AB; inspection certificate 3.2 no. 6610/300425080, heat no. 571820-001. The sheets were delivered in the as-supersaturated state (from a temperature of 1040 °C). The chemical composition of steel 1.4462 based on the PN-EN 10088-2 standard and inspection certificate 3.2 are presented in Table 4.

Table 5 presents the mechanical properties of steel 1.4462 in accordance with the PNEN 10088-2 standard and inspection certificate 3.2.

The filler metal used in the tests was an AVESTA 2205 solid electrode wire having a diameter of 1.2 mm (G 22 9 3 N L in accordance with PN-EN ISO 14343, ER 2209 in accordance with AWS A5.9). The chemical composition of the filler metal wire is presented in Table 6, whereas its mechanical properties are presented in Table 7.

The shielding and backing gas used in the tests was CRONIGON® He20 (M12-ArHeC-20/2 in accordance with PN-EN ISO 14175) composed of CO_2 (2 %), He (20 %) and Ar (78 %). The flowrate of the (weld face) shielding gas amounted to 12 l/min, whereas the flowrate of the (weld root) backing gas amounted to 6 l/min.

2.6. Test and measurement stations

2.6.1. Test station characteristics

The test station (Fig. 2) was provided with a TAWERS WG3 welding power source featuring a control panel, a TA-1800 welding robot (PANASONIC), positioners, a turntable, an active filler metal wire feed system, fixtures enabling the fixing of test specimens and computers recording energy-related parameters (necessary for calculating linear energy).

Table 4. Chemical composition of duplex steel 1.4462

	C	Si	Mn	P	S	Cr	Ni	Mo	Nb	Cu	Co	N
	[wt %]											
Requirements in accordance with PN-EN 10088-2	max. 0.03	max. 1.00	max. 2.00	max. 0.035	max. 0.015	21.0–23.0	4.50–6.50	2.50–3.50	–	–	–	0.10–0.22
Requirements in accordance with inspection certificate 3.2	0.02	0.44	1.34	0.029	0.001	22.22	5.69	3.13	0.007	0.28	0.160	0.167

Table 5. Mechanical properties of duplex steel 1.4462

	R_m [MPa]	$R_{p0.2}$ [MPa]	A [%]	HB
Requirements in accordance with PN-EN 10088-2	700–950	min. 500	min. 20	max. 271
Requirements in accordance with inspection certificate 3.2	848	655	30	252

Table 6. Chemical composition of the filler metal wire (AVESTA 2205) [27]

C	Si	Mn	Cr	Ni	Mo	N	PRE_N
[wt %]							
≤ 0.015	0.40	1.70	22.50	8.80	3.20	0.15	≥ 35

Table 7. Mechanical properties of the filler metal wire (AVESTA 2205) [27]

FN	R_m [MPa]	$R_{p0,2}$ [MPa]	A [%]	KV [J]	
				+20 °C	−40 °C
50	830 (≥ 550)	660 (≥ 450)	28 (≥ 20)	85	≥ 32

2.6.2. Station for non-contact measurements of welding strains

Non-contact measurements of welding strains (deformations) were performed using a 3D ATOS III Triple Scan scanner (GOM GmbH) and ATOS Professional software (Fig. 3).

The scanner used in the tests (3D ATOS III Triple Scan) is an advanced optical measurement system based on the method of blue structural light projection (also known as digital light projection – DLP). The system, whose principle of operation is based on triangulation, consists of a projector and two digital cameras, positioned at an appropriate angle. During the measurement, the projector projects patterns composed of fringes onto the object being measured, whereas the two cameras record the course of the fringes, enabling the creation of a 3D image in one shot. By solving the optical transformation equations, the system calculates the coordinates for each camera pixel with a previously specified accuracy. Measurements are recorded in the form of points in space described by XYZ coordinates (the so-called cloud of points) in the coordinate system of the object. The number of scans depends on the complexity of an element subjected to scanning and may contain between several and tens of millions of points. When measuring a given element, the system compiles individual clouds of points based on reference points, the distances between which do not change during measurements. The result of measurements is the spatial representation of the surface in the form of a combined cloud of points (having a common coordinate system).

The measurements are followed by the process of polygonisation, during which the cloud of points is transformed into appropriate areas (individual measured points are connected to form a mesh of triangles). Such a model is

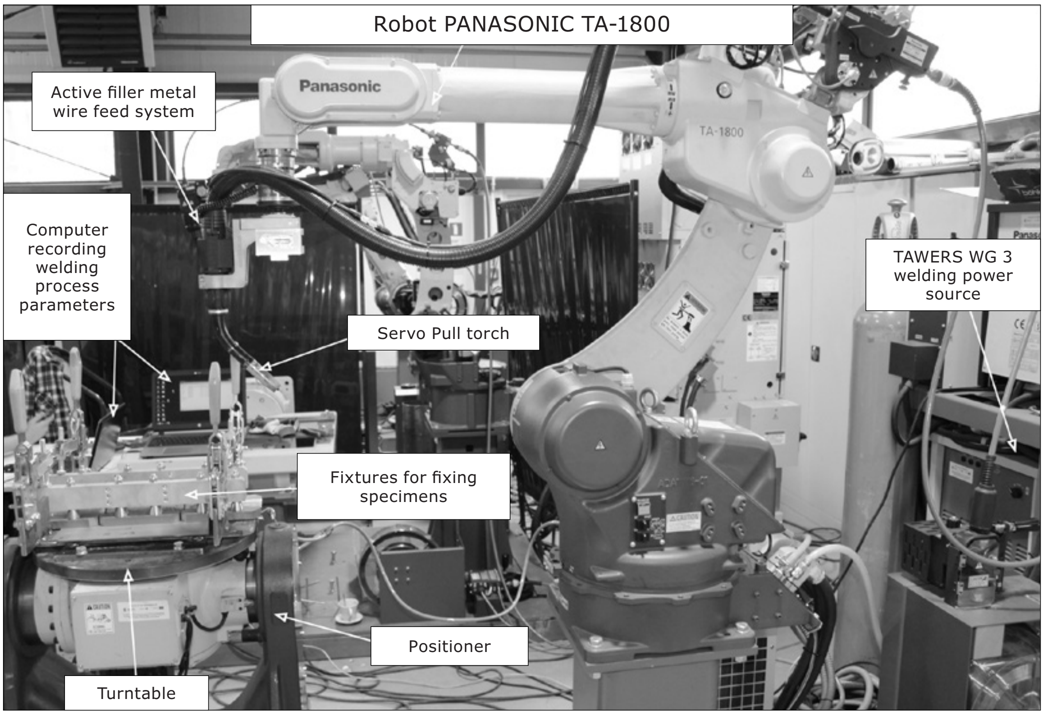

Fig. 2. Robotic testing station equipped with the TAWERS welding system

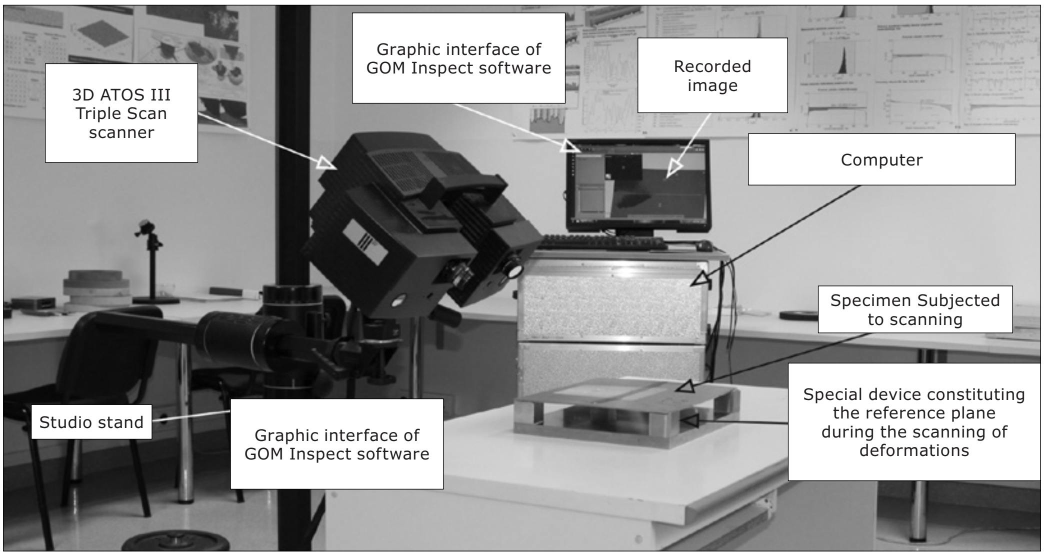

Fig. 3. Station for non-contact measurements of welding strains equipped with a 3D ATOS III Triple Scan scanner (GOM)

subjected to dimensional analysis, where the system compares data collected from the object subjected to scanning with a related CAD model. The results of the above-named comparison can be presented in the form of tables and colour maps, with deviations from the nominal dimension (dimension from the CAD model) [28, 29].

2.7. Test joints

The test involved the preparation of 40 specimens (3 mm × 150 mm × 350 mm), in accordance with the PNEN ISO 15614 standard, out of which 20 test joints were made. Because of the anisotropy of mechanical properties (elongated grains and the crystallographic structure formed during rolling), the specimens were cut out with their longer edge being parallel to the direction of rolling (of the sheets).

In order to limit the heat input to the base material, the specimens were cut out using the abrasive-water jet (AWJ) and subjected to milling-based finishing.

The welding of the test joints was compared by performing measurements and recording process energy parameters, i.e. current and arc voltage (based on signals transmitted from the measurement system of the TAWERS welding system). Data acquisition was performed at a frequency of 6667 Hz.

3. Test results and discussion

3.1. Assessment of the effect of welding process linear energy on welding strains

Measurements of local flatness deviations, i.e. distances between the actual surface and the measurement plane determined using the least squares method, at points in area A having coordinates (x, y), were performed in accordance with the PN-EN ISO 13920:2000 standard, applying an appropriate non-contact method.

Flatness deviations were assessed using a parameter referred to as the mean square deviation of surface flatness. The parameter, designated as *FLTq*, is calculated in accordance with equation (2) [30]:

$$FLTq = \sqrt{\frac{1}{A}\int_A \Delta FLT^2 \, dA}, \qquad (2)$$

where ΔFLT – local flatness deviation determined in relation to the reference plane, the value of which is equal to the distance from the point located on the actual surface to the reference plane and perpendicular to the reference plane and A – surface area, for which the joint flatness is determined.

Table 8 presents the distribution of flatness deviations of the test joints made of steel 1.4462 using the MAG (DC+) method and various values of linear energy.

In butt joints of thin elements characterised by low stiffness (such as the test joints), transverse shrinkage (contraction) is responsible for the loss of flatness. The analysis concerning the calculated values of the mean square deviation of surface flatness *FLTq* (based on non-contact measurements) indicated the usability of the method in the determination of welding strains (deformations).

The correlation between the heat input to the joint (linear welding energy *Q*) and the size of welding strains (deformations), determined by the value of the mean square deviation of surface flatness *FLTq*, is presented in Figure 4. The figure contains a trend line indicating that an increase in the value of linear energy triggered an increase in the value of welding strains. The value of the coefficient related to the determination of trend line $R^2 = 0.7929$ indicates the satisfactory matching of exponential regression equation (3) to experimental data within the variability range of primary process parameters:

$$FLTq = 0.1805 \exp(8.7262Q) \qquad (3)$$

where $FLTq$ – mean square deviation of surface flatness [mm]
Q – linear welding energy [kJ/mm]

Table 8. Distribution of flatness deviations of the test joints made of steel 1.4462 using the MAG (DC+) method and various values of linear energy.

Spec. no.	Linear energy *Q* [kJ/mm]	Mean square deviation of surface flatness *FLTq* [mm]	Deformation assessment – comparison of the actual element and the CAD model – map of deviations
1	0.2208	1.488	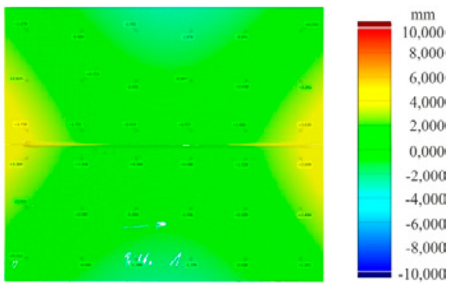
2	0.3496	5.075	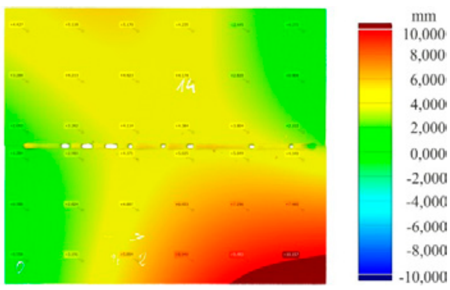

Table 8. Continued

Spec. no.	Linear energy *Q* [kJ/mm]	Mean square deviation of surface flatness *FLTq* [mm]	Deformation assessment – comparison of the actual element and the CAD model – map of deviations
3	0.2398	1.076	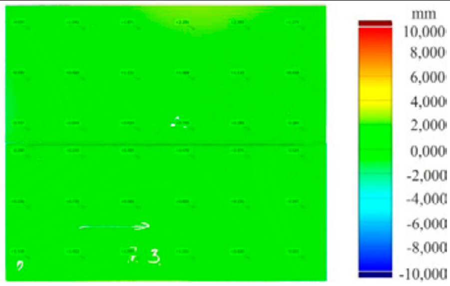
4	0.4070	5.382	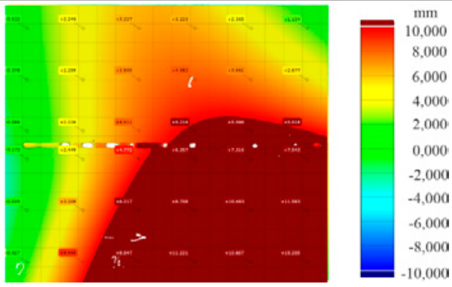
5	0.1393	0.639	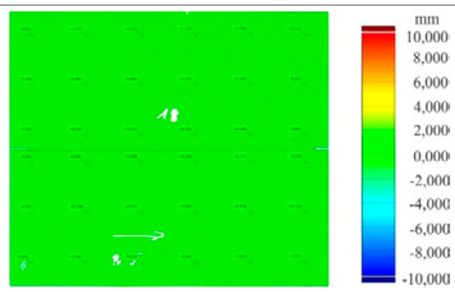
6	0.2149	3.192	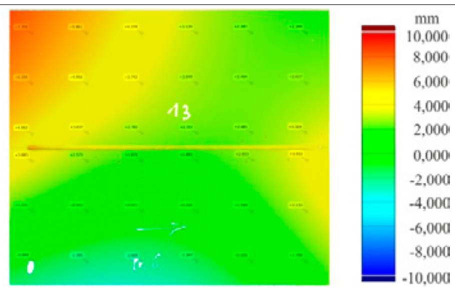
7	0.1548	0.654	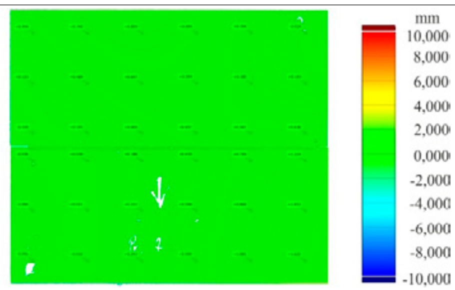
8	0.2854	1.895	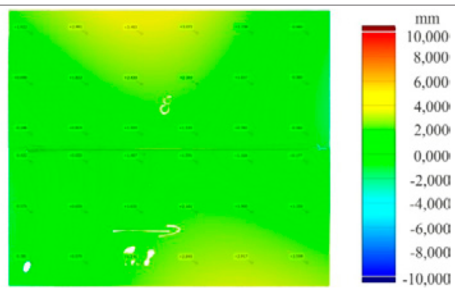

Table 8. Continued

Spec. no.	Linear energy *Q* [kJ/mm]	Mean square deviation of surface flatness *FLTq* [mm]	Deformation assessment – comparison of the actual element and the CAD model – map of deviations
9	0.3196	4.352	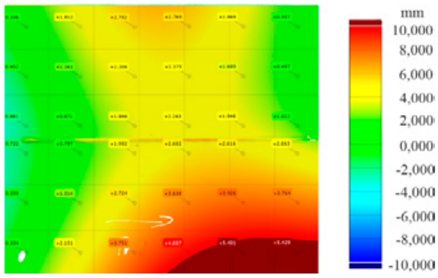
10	0.1395	0.451	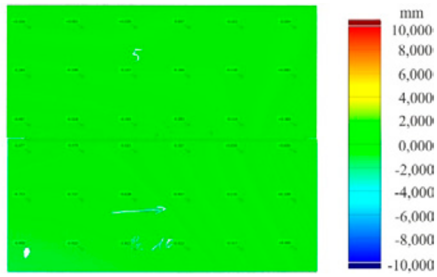
11	0.2807	1.382	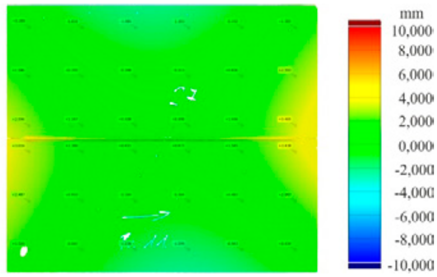
12	0.1869	1.014	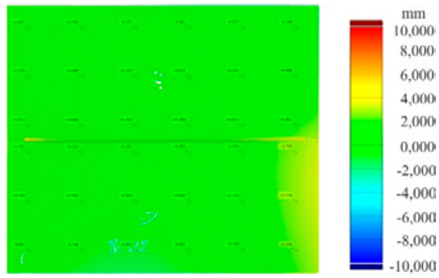
13	0.2256	1.337	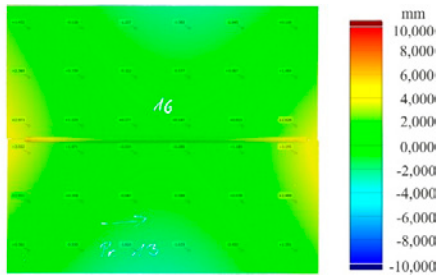
14	0.3262	1.417	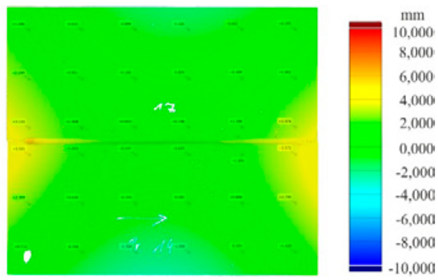

Table 8. Continued

Spec. no.	Linear energy *Q* [kJ/mm]	Mean square deviation of surface flatness *FLTq* [mm]	Deformation assessment – comparison of the actual element and the CAD model – map of deviations
15	0.2485	1.430	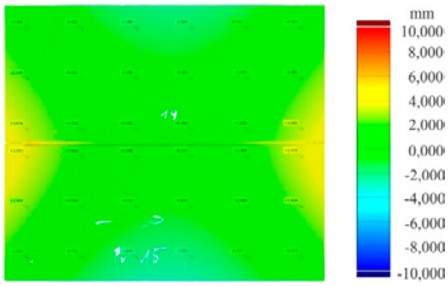
15_1	0.2484	1.429	
15_2	0.2486	1.431	
15_3	0.2485	1.430	
15_4	0.2483	1.426	
15_5	0.2484	1.427	

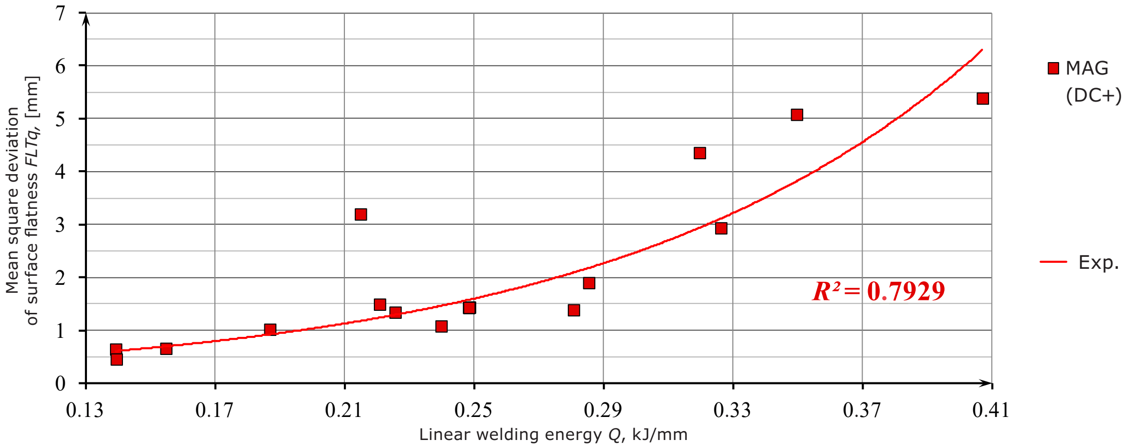

Fig. 4. Correlation between mean square deviation of surface flatness *FLTq* and linear welding energy *Q* of the test joints made of steel 1.4462 using the MAG (DC+) method along with the trend line

It should be noted that linear energy (which is a generalised parameter set in the welding process) is calculated in accordance with the functional dependence (1) based on the measured values of input parameters, i.e. arc voltage, current and welding rate, having various effects on the value of the aforesaid energy. The effect of the product of arc voltage and current is directly proportional to the inverse of the welding rate. As a result, it is possible to obtain the same linear energy in relation to different combinations of the values of the above-named input parameters. The effect of input process parameters on the size of welding deformations varies as well.

Taking the foregoing into consideration and experimental data, using the Statistica ver. 13 software programme and Experiment Planner 1.0.1, it was possible to determine the equation of regression describing the dependence of mean square deviation of surface flatness *FLTq* on the preset values of welding process parameters, adopting the model of dependence in the form of an exponential function with an exponent having the form of the first-degree algebraic polynomial with interactions, having the following form (4):

$$FLTq = \exp(25.98 - 0.1903I - 1.332U - 2.0902v + 0.0103IU + 0.0218Iv - 0.001034IUv) \quad (4)$$

where $FLTq$ – mean square deviation of surface flatness [mm]
U – preset arc voltage [V]
I – preset welding current [A]
v – preset welding rate [mm/s]

The coefficient of determination R^2 = 0.9302 indicated the proper match of the exponential regression equation to the experimental data:

- mean value of all measurements: 1.907;
- mean value of mathematical model results: 1.8619.

The significance of determination coefficient R^2 was verified using the *F*-test (Wald test):

- value of test function: $F = 11.0123$,
- critical value of F_{cr} statistic in relation to significance level $\alpha = 0.05$: $F_{cr} = 2.91$.

Because of the fact that inequality $F > F_{cr}$ took place, there were no grounds for the rejection of the hypothesis concerning the significance of the determination coefficient. In other words, the model was adequate for experimental results in relation to assumed significance level $\alpha = 0.05$ (the total significance of variables was maintained). Assessment (based on using the Student's t-test) was also performed in relation to the significance of regression function terms. The results of the calculations are presented in Table 9.

The calculations revealed that all the calculated coefficients of the equation were significant and should be used in regression equation (4).

The determination of the mathematical model describing the process under investigation was followed by the preparation of related diagrams. Figures 5–7 present diagrams concerning the mathematical model of mean square deviation of surface flatness *FLTq* determined on the basis of experimental tests in relation to the preset values of welding process input parameters, i.e. current, arc voltage and welding rate.

Table 9. Significance of the terms of the regression function describing the dependence of the mean square deviation of surface flatness and the preset values of welding process input parameters

Symbol	Value of regression function term	Value of the Student's t-test	Critical value of the Student's t-test	Significance of regression function term
(0)	25.98	2.859	2.179	Yes
I	−0.1903	2.881	2.179	Yes
U	−1.332	3.097	2.179	Yes
v	−2.902	3.254	2.179	Yes
IU	0.01033	3.305	2.179	Yes
Iv	0.02177	3.359	2.179	Yes
Uv	0.1321	3.131	2.179	Yes
IUv	−0.001034	3.37	2.179	Yes

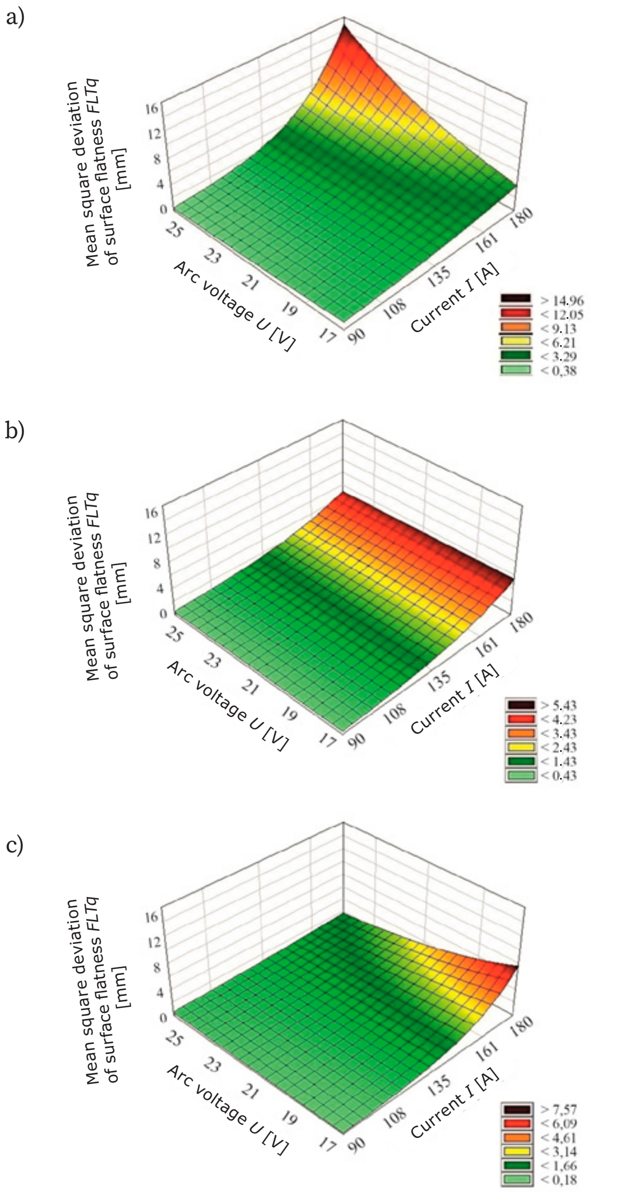

Fig. 5. Diagrams of the mathematical model of the mean square deviation of surface flatness *FLTq* determined on the basis of experimental tests as a function of changes in values of current and arc voltage in relation to: a) welding rate $v = 6.67$ mm/s (minimum), b) welding rate $v = 10$ mm/s (mean) and c) welding rate $v = 13{,}33$ mm/s (maximum)

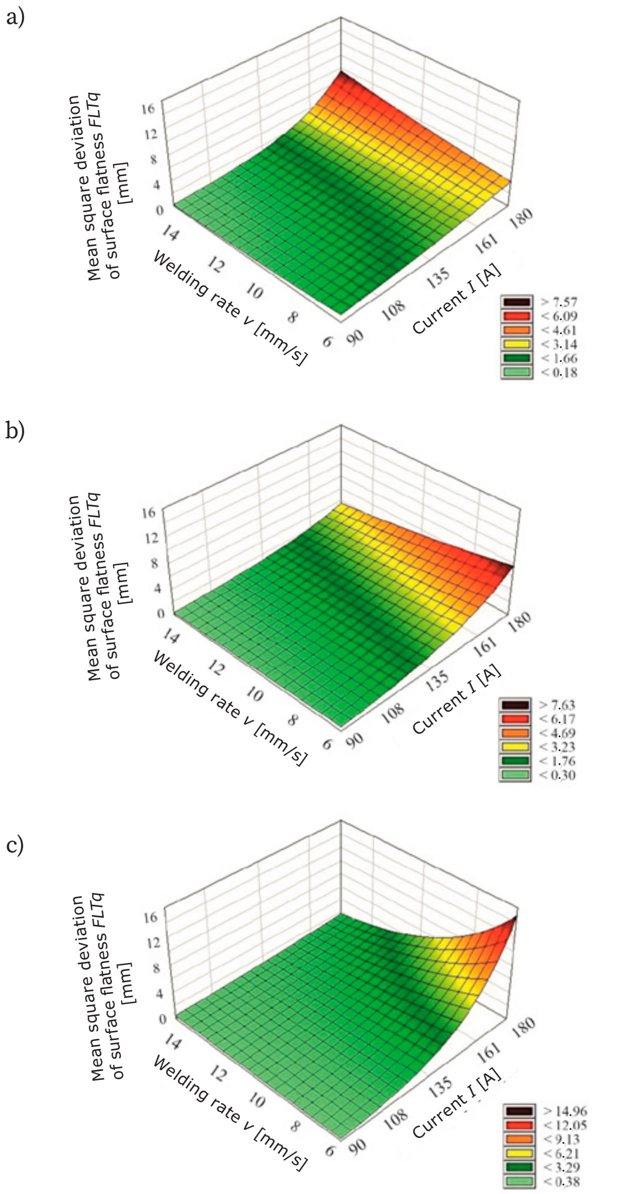

Fig. 6. Diagrams of the mathematical model of the mean square deviation of surface flatness FLTq determined on the basis of experimental tests as a function of changes in values of current and welding rate in relation to: a) arc voltage U = 17 V (minimum), b) arc voltage U = 21 V (mean) and c) arc voltage U = 25 V (maximum)

Function (4) constitutes a mathematical model identifying the values of the mean square deviation of surface flatness in the MAG (DC+) welding of joints made of ferritic-austenitic steel grade 1.4462 in accordance with the PN-EN 10088-2 standard, under specific welding conditions, in relation to significance level $\alpha = 0.05$. The analysis of the model revealed its usability in explaining (and forecasting) the size of welding strains (deformations) in relation to the values of welding process input parameters.

The experimental tests revealed the existence of a narrow range of the heat input, in relation to which welding strains (deformations) were significantly smaller than those formed in relation to the remaining heat input values. The dependence of welding strains on the heat input to the material during welding was not a monotonic function. The range of permissible welding parameter values could be determined by making test joints using variable welding parameters, followed by the scanning of finished joints using a 3D scanner and analysing the size of deformations.

a) b) c)

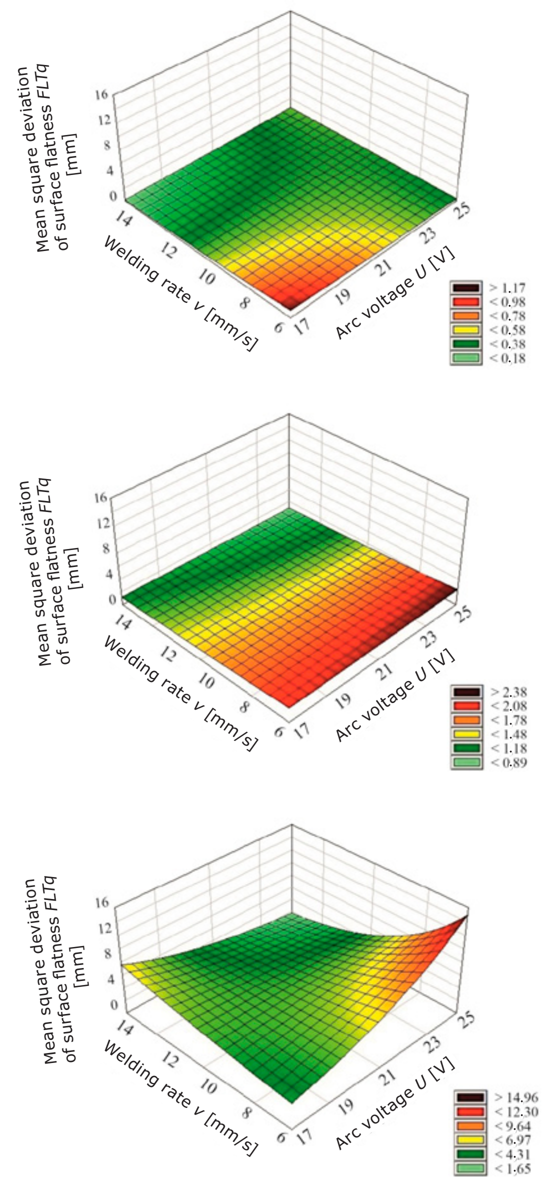

Fig. 7. Diagrams of the mathematical model of the mean square deviation of surface flatness FLTq determined on the basis of experimental tests as a function of changes in values of arc voltage and welding rate in relation to: a) current I = 90 A (minimum), b) current I = 135 A (mean) and c) current I = 180 A (maximum)

4. Summary and conclusions

The research-related tests involved the assessment of the macrostructure and deformations of arc-welded joints made of ferritic-austenitic steel (duplex). The results of the tests justified the formulation of the following detailed conclusions:

1. Linear energy, being a generalized parameter set in the welding process, is calculated in accordance with functional dependence (1) and on the basis of arc voltage, current and welding rate, having various effects on the value of energy. The effect of the product of arc voltage value and current (current power) is directly proportional to the inverse of the welding rate. As a result, it is possible to obtain the same value of linear energy using various combinations of the values of the above-named input parameters.
2. Non-contact measurements of welding strains and their subsequent analysis in relation to the reference element (e.g. CAD model) enabled the identification of welding process-triggered changes in dimensions and deformations of joined elements.
3. The results of welding strain measurements made it possible to determine the regression equation describing the correlation between welding strains (determined by the value of the mean square deviation of surface flatness) and preset values of welding process input parameters, i.e. current, arc voltage and welding rate.
4. Because of the process complexity and the large number of variable factors undergoing complex interactions, welding is not an entirely repeatable (reproducible) process. Many factors influence the final effect (i.e. the quality of the joint), yet the application of similar welding conditions minimises the risk of welding imperfection formation. It is not possible to develop a mathematical model of the welding process solely using statistical methods; it is only possible to determine parameter values ensuring the obtainment of the highest quality according to previously defined criteria.
5. The analysis of mathematical models revealed their usability in explaining (and forecasting) the size of welding deformations in relation to values of welding process input parameters.
6. The determination of the regression function and the development of its three-dimensional diagram (response area) could be the starting point for the optimisation of welding process parameters.
7. The application of dependences determined within the above-presented tests is limited to the range of variability of the factors subjected to the tests and the necessity of ensuring the stability of arc burning as well as the fabrication of joints meeting specific acceptance criteria, including quality levels of welded joints and their mechanical properties.

REFERENCES

[1] Klimpel A.: Spawanie, zgrzewanie i ciecie metali. Technologie. Wydawnictwo Naukowo-Techniczne, Warszawa 1999.

[2] Myśliwiec M.: Cieplno-mechaniczne podstawy spawalnictwa. Wydawnictwo Naukowo-Techniczne, Warszawa 1970.

[3] Tasak E.: Metalurgia spawania. Wydawnictwo JAK, Kraków 2008.

[4] Baddoo N.R.: Stainless Steel in Construction: A Review of Research, Applications, Challenges and Opportunities. Journal of Constructional Steel Research, 2008, vol. 64, pp. 1199–1206.
[5] Balachandran G., Balasubramanian V.: Stainless Steel Processing to Meet Advanced Applications. Advanced Materials Research, 2013, vol. 794, pp. 135–158.
[6] Lo K.H., Shek C.H., Lai J.K.L.: Recent developments in stainless steels – Reports. Materials Science and Engineering, 2009, vol. 65, pp. 39–104.
[7] Venkatraman M., Pavitra K., Jana V., Kachwala T.: Manufacturing and Critical Applications of Stainless Steel – An Overview. Advanced Materials Research, 2013, vol. 794, pp. 163–173.
[8] Nowacki J.: Stal dupleks i jej spawalność. Wydawnictwo Naukowo-Techniczne, Warszawa 2009.
[9] Singh J., Goswami N.: Welding of Duplex Stainless Steel. International Journal for Scientific Research & Development, 2013, vol. 1, no. 4, pp. 919–925.
[10] Krauss G.: Steels. Processing, Structure and Performance, Second Edition, ASM International, Materials Park, Ohio, USA 2015. ISBN: 978-1-62708-083-5.
[11] Dabalà M., Calliari I., Variola A.: Corrosion behavior of a superduplex stainless steel in chloride aqueous solution. Journal of Materials Engineering and Performance, 2004, vol. 13, no. 2, pp. 237–240. DOI.org/10.1361/10599490418316.
[12] Kim S.J., Ko S.H., Kang K.H., Han J.: Direct seawater desalination by ion concentration polarization. Nature nanotechnology, 2010, vol. 5, pp. 297–301. DOI: 10.1038/nnano.2010.34.
[13] Practical Guidelines for the Fabrication of Duplex Stainless (3rd edition). International Molybdenum Association (IMOA), London, UK 2014. ISBN 978-1-907470-09-7.
[14] Van der Mee V.: Spawanie stali odpornych na korozję o strukturze dwufazowej. Biuletyn Instytutu Spawalnictwa, 2016, vol. 60, no. 5, pp. 44–55. https://doi.org/10.17729/ebis.2016.5/6.
[15] Pilarczyk J. (red.): Poradnik inżyniera – Spawalnictwo, vol. 1, Wydawnictwo Naukowo-Techniczne, Warszawa 2003.
[16] Ferenc K.: Spawalnictwo. Wydawnictwa Naukowo-Techniczne, Warszawa 2007.
[17] Gunn R.N. (ed.): Duplex stainless steel. Microstructure, properties and applications. Abington Publishing, Cambridge 1997. ISBN: 1 85573 318 8.
[18] Nowacki J.: Stal duplex i jej spawalność. Przegląd Spawalnictwa, 2008, vol. 10, pp. 34–44.
[19] Avery R.E.: Resist chlorides retain strength and ductility with duplex stainless steel alloys. Chemical Engineering Progress, 1991, vol. 87, pp. 78–82.
[20] Nilsson J.O., Huhtala T., Jonsson P., Karlsson L., Wilson A.: Structural stability of super duplex stainless wells metals and its dependence on tungsten and copper, Metallurgical and Materials Transactions A, 1996, vol. 27, no. 8, pp. 2196–2208. https://doi org/10.1007/BF02651874.
[21] Nowacki J., Urbański M., Zając P.: Spawanie FCAW stali duplex w budowie statków do transportu chemikaliów. Przegląd Spawalnictwa, 2008, vol. 4, pp. 3–10.
[22] Karlsson L.: Welding duplex stainless steel – A review of current recommendations. Welding in the World, 2012, vol. 56 (5), pp. 65–76. https://doi.org/10.1007/BF03321351
[23] Maslak M., Stankiewicz M., Slazak B.: Duplex Steels Used in Building Structures and Their Resistance to Chloride Corrosion. Materials, 2021, vol. 14, pp. 5666. https://doi.org/10.3390/ma14195666.
[24] PN-EN 1011-1: 2009: Spawanie – Wytyczne dotyczące spawania metali – Część 1: Ogólne wytyczne dotyczące spawania łukowego.
[25] ISO/TR 17671-1: 2002: Welding – Recommendations for welding of metallic materials – Part 1: General guidance for arc welding.
[26] Kukiełka L.: Podstawy badań inżynierskich. Wydawnictwo Naukowe PWN, Warszawa 2002.
[27] Avesta 2205 Welding wire: Specyfikacja produktu. Böhler Welding, 2014.
[28] Allard P., Lavoie J.: Differentiation of 3D scanners and their positioning method when applied to pipeline integrity. EITEP Institute, 2014.
[29] Information materials of GOM, http://www.gom.com [access date: 14.08.2020].
[30] Adamczak S.: Pomiary geometryczne powierzchni. Wydawnictwo NaukowoTechniczne, Warszawa 2008.
[31] Kik T.: Predykcja własności złączy spawanych z wykorzystaniem zaawansowanych modeli źródeł ciepła. Wydawnictwo Politechniki Śląskiej, Gliwice 2022.